18TH WORLD CONFERENCE ON EARTHQUAKE ENGINEERING
WCEE2024
MILAN

MILAN, ITALY
30TH JUNE - 5TH JULY 2024

www.wcee2024.it

COMPARISON OF STRUCTURAL DEMANDS FOR REAL, SCALED, SPECTRAL-MATCHED AND ARTIFICIAL ACCELEROGRAMS

C. Cantagallo[1], M. Terrenzi[1], E. Spacone[1] & G. Camata[1]

[1] University "G d'Annunzio" of Chieti-Pescara, Department of Engineering and Geology, Pescara, Italy, e-mail: {cristina.cantagallo, marco.terrenzi, espacone, guido.camata}@unich.it

Abstract: *One of the major sources of uncertainty in Nonlinear Response History Analyses (NRHAs) is the selection of the ground motion records. Different sets of ground records can in fact produce different structural demands, each characterized by its own variability level. In this work the structural demands computed from four typologies of records are compared: real unscaled records, linearly scaled records, spectral-matched records adjusted by wavelets and artificial records. The ground motion records are selected for the seismic hazard corresponding to the return period of 475 years. Each set of records consists of 20 pairs of ground motion records spectrum-compatible according to Eurocode 8. First, the energy content of the selected ground motion records is calculated for each set of accelerograms. The energy parameters of the modified set of records are related to the corresponding real ground motions in order to evaluate the variation of the seismic input induced by the records' modification. NRHAs of two 6-storey existing reinforced concrete buildings are then carried out using the selected records. The two buildings have a structural scheme with and without masonry infills, respectively. Finally, the structural demands obtained with all modified sets of records are compared with those obtained with real accelerograms.*

1 Introduction

The increased computing capabilities of current computer software make it possible to apply Nonlinear Response History Analyses (NRHAs) to different types of structures to evaluate their ultimate behaviour under seismic loads using refined models. Nevertheless, the variability of these complex computations strongly depends on the input ground motions (Cantagallo et al., 2014), whose selection can generate important discrepancies in the results and therefore difficulties to deal with for engineering purpose.

This paper focuses on evaluating the differences in seismic demands obtained using different sets of input ground motion records, and specifically: (a) real unscaled ground motion records (RR), (b) linearly scaled ground motion records (LSR), (c) spectral-matched ground motion records (SMR) and (d) artificial accelerograms (AA).

The modifications of the real ground motion records carried out in sets (b) and (c) or the generation of artificial accelerograms in set (d) can lead to seismic ground motion inputs with significantly high energy contents (Romanelli et al., 2023). To verify this statement, the energy-based Ground Motion Parameters (GMPs) were obtained first for each considered set of ground motions, followed by the comparison between the GMPs before and after the modification process. The GMPs of artificial accelerograms were compared with the average value obtained from RR.

A total of 160 NRHAs were carried out on an existing six-storey reinforced concrete (RC) building with and without masonry infills by using the above sets of ground motion inputs. Finally, the comparison between the seismic demands obtained using modified or artificial accelerograms (SMR or AA) and real or linearly scaled ground motion records (RR or LSR) was carried out to evaluate the change in seismic demand obtained with the spectral matching process or with the artificial generation of time histories.

2 Case study structures

The case study building used in this work is a six-storey existing structure designed for gravity loads only according to an old Italian code (DM 30/05/1974). As shown in Figure 1, the plan layout is rectangular and all interstorey heights are equal to 3.2 m. The floors consist of cast-in-place RC joists separated by lightweight hollow clay bricks and topped by a 4 cm thick concrete slab. The frames layout provides a regular distribution of stiffness and strength. The building was designed following allowable stress design principle prescribed by the Italian DM 30/05/1974. Dead and live loads on structural elements were calculated using the nominal values given in DM 16/01/1996.

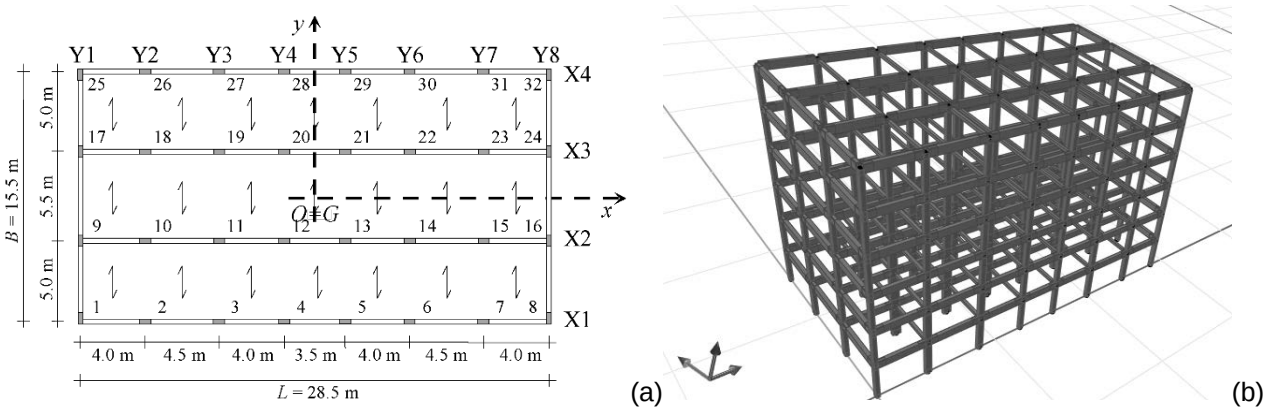

Figure 1. Case study building plan view (a) and 3D model (b).

The analyses were carried out with the computer software OpenSees (McKenna et al., 2010) with the pre- and post-processor STKO (Petracca et al., 2017). The model was defined using Beam-with-Hinges elements (Scott and Fenves, 2006) with end sections (hinges) of assigned length for all structural members. The end hinges were modelled using fibre sections (Spacone et al., 1996) with length equal to the cross-section depth: for non-square columns, this length is the average of the cross-section depths. The central parts of the Beam-with-Hinges elements were modelled as linear elastic (Terrenzi et al., 2020). The concrete and steel fibres were modelled using the constitutive laws Concrete01 (Kent and Park, 1971) and Steel01 (Mazzoni et al., 2006), respectively. For Steel01, E_s = 206000 *MPa*, f_y = 400 *MPa* and strain-hardening ratio b = 0.0049. For concrete, f_{pc} = 28 *MPa*, ε_{c0} = 2.5‰, f_{pcu} = 20% f_{pc} and ε_{cu} = 3.5‰, where symbols are those used in the OpenSees Manual (Mazzoni et al., 2006). Confined concrete was not considered because it is assumed that the stirrup spacing is too large for an effective confinement and the stirrups have 90° rather than 135° hooks. A rigid diaphragm was considered at each floor. However, since this constraint restrains axial deformations in the beams, it also introduces spurious axial (generally compression) forces. For this reason, an axial buffer (zero-length) element (Barbagallo et al., 2020) with very low axial stiffness was introduced at one end of each beam. The structural model considers ductile mechanisms only and neglects brittle mechanisms such as shear failures. The focus of the study is on the effect of ground motion selection on the structural demand using different types of ground motions and the modelling of brittle mechanisms would significantly increase convergence problems and computational times.

The case study structure was modelled with and without masonry infills and the two so-defined structural models were named "infilled structure" and "bare structure", respectively. Masonry infills were modelled with an equivalent strut with the phenomenological model proposed by Decanini et al. (1987) and later enhanced by Cardone and Perrone (2015) and Sassun et al. (2016). This model describes both the monotonic and cyclic behavior of the masonry infills and considers the presence of openings too. At the ground floor the external rear frame is infilled without openings, while on the other sides there are no infills. At the other floors all the

external frames are infilled, with different percentages of openings ranging from approximately 0% to 80%. The infills distribution provides a significant asymmetry both in plan and elevation.

Table 1 reports the periods and the mass participation ratios of the first three modes (computed after application of the gravity loads) of the bare and infilled structure. T[s], Mx[%], My[%] and Rz[%] are the period of vibration, the x-direction, the y-direction and the z-direction rotational mass participation ratios, respectively. The participating masses show that the first three modes of the bare structure are uncoupled, with translational first and third modes while the second mode is torsional. In the infilled structure, the second and third modes are strongly coupled due to the eccentricity provided by the infills distribution.

Table 1. First three vibration modes of the bare and infilled structure after gravity load application.

Bare Structure			
T [s]	**Mx [%]**	**My [%]**	**Rz [%]**
2.59	0	78.65	0
1.48	0	0	80.45
1.20	79.34	0	0

Infilled structure			
T [s]	**Mx [%]**	**My [%]**	**Rz [%]**
0.97	0	93.56	0
0.64	70.21	0	19.50
0.53	15.45	0	74.51

3 Ground motion record selection

3.1 Real unscaled ground motion records

A set of 20 pairs of real ground motion records (RR) is selected from two databases, the European Strong-motion Database ESD (Ambraseys et al., 2004) and the Engineering Strong-Motion database ESM (Luzi et al., 2016). The number of ground motion records included in each set is such that the multi-directionality of the seismic input can be neglected (Cantagallo et. al. 2015; Skoulidou and Romão, 2020; Cantagallo et al. 2023). The selection is carried out according to the spectrum-compatibility criterion provided in Eurocode 8 (CEN, 2005) that states that in the $0{,}2T_1$ - $2T_1$ range of periods, no value of the average elastic spectrum should be less than 90% of the corresponding Uniform Hazard Spectrum (UHS). For this study, a 110% upper bound is added to the previous lower bound. Following Beyer and Bommer (2006), a single response spectrum $S_a(T)$ is calculated from the response spectra of the two horizontal ground motion components S_{aX} and S_{aY}:

$$S_a(T) = \sqrt{S_{aX}(T) \cdot S_{aY}(T)} \quad (1)$$

The record selection is carried out for a probability of exceedance of 10% in 50 years (T_R = 475 years) and a reference site located on rock soil at L'Aquila (AQ-Italy) - 42.350° latitude and 13.399° longitude.

Figure 1a and Figure 1b show the spectrum-compatibility criterion applied to the bare and the infilled structure, respectively. Each plot reports the response spectra of the single real records (grey lines), the average spectrum (red line), the UHS (black lines), the 90% and the 110% bounds (dashed black lines) and the spectrum-compatibility range (dotted vertical black lines) considered for the ground motion selection of RR. Note that for the bare structure, the spectrum compatibility range is between 0.52 sec and 5.2 sec (Figure 1a), while for the infilled structure it is between 0.19 sec and 1.94 sec (Figure 1b) thus the x (period) range of the two plots is considerable different.

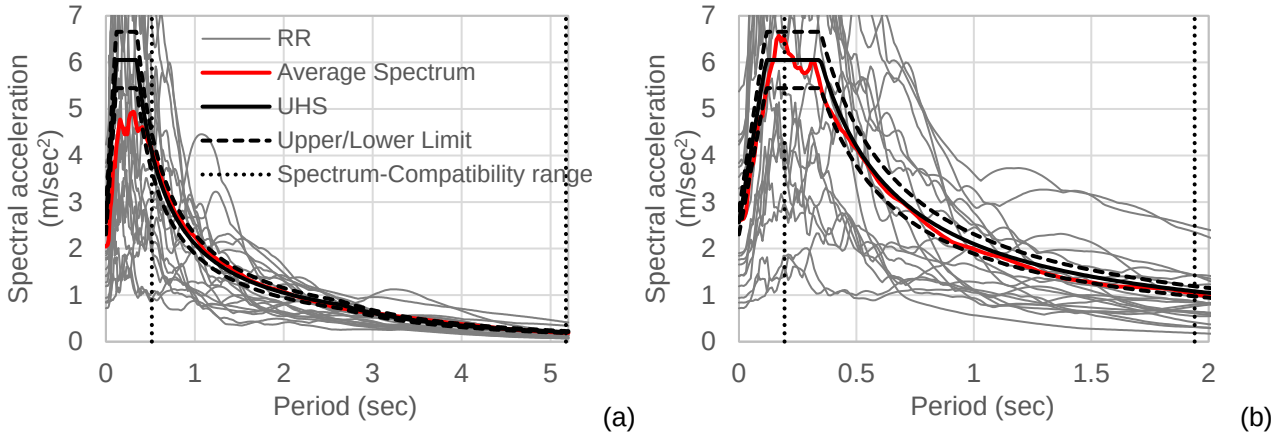

Figure 2. Geometric response spectra, average response spectrum, UHS, upper (110%) and lower (90%) spectrum-compatibility bounds and spectrum-compatibility ranges (vertical lines) of the 20 RR selected for the bare structure (a) and the infilled structure (b).

3.2 Modified ground motion records

Linearly scaled ground motion records

A set of 20 pairs records scaled to the first vibration period T_1 of each structure is selected according to the same spectrum-compatibility criterion used for the RR. In order to satisfy this criterion, the sets of ground motion records included in RR and LSR are different. Figure 2a and Figure 2a show the LSR selected for the bare structure (a) and the infilled structure (b), respectively.

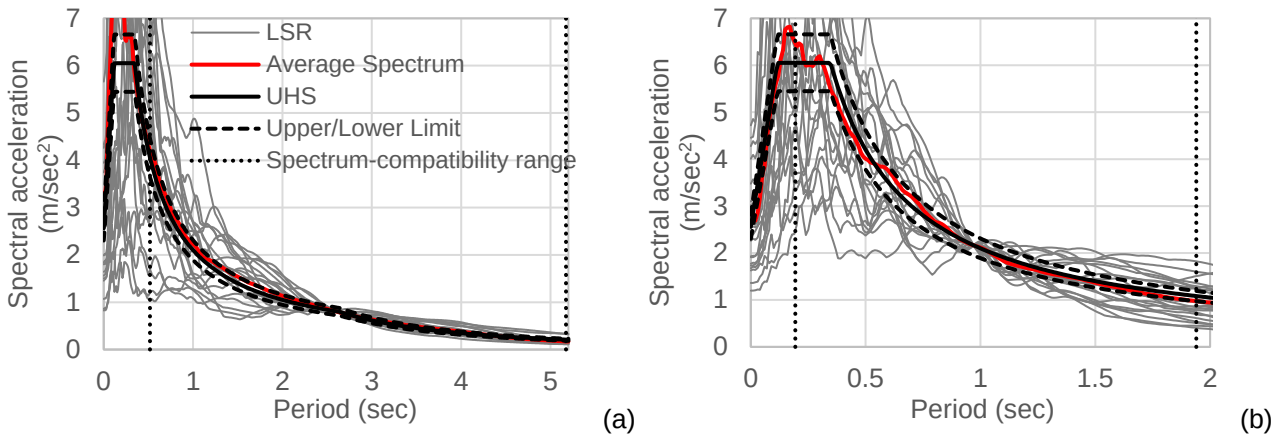

Figure 3. Geometric response spectra, average response spectrum, UHS, upper (110%) and lower (90%) spectrum-compatibility bounds and spectrum-compatibility ranges of the 20 LSR selected for the bare structure (a) and the infilled structure (b).

Spectral matched records

The twenty pairs of RR and LSR were matched to the UHS to obtain spectral matched records defined SMR-RR and SMR-LS, respectively. The matching process is based on the selective application of wavelet transforms on the spectrum of the signal to match the UHS (Hancock, 2006). This operation reduces the variability of structural demand. The spectral matching was carried out in this work with the software SeismoMatch (2022) using the wavelet algorithm proposed by Al Atik and Abrahamson (2010). Figure 3a and Figure 3b show the application of the spectrum-compatibility criterion applied to the SMR-RR selected for the bare structure and the infilled structure, respectively. Similar plots could be drawn for SMR-LS.

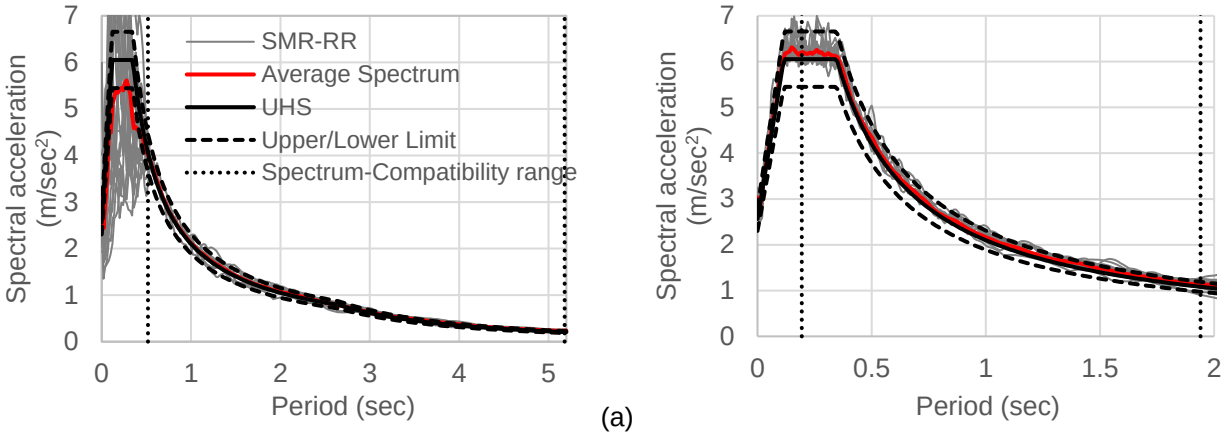

(a)

Figure 3. Geometric response spectra, average response spectrum, UHS, upper (110%) and lower (90%) spectrum-compatibility bounds and spectrum-compatibility ranges of the 20 SMR-RR obtained for the bare structure (a) and the infilled structure (b).

3.3 Artificial accelerograms

According to Eurocode 8 (CEN, 2005), artificial accelerograms have to be generated so as to match the UHS. The compatibility with the considered spectrum is controlled following the same spectrum-compatible criterion used for RR and SMR.

The artificial (or generated) accelerograms were obtained in this work using the software SIMQKE_GR (Gelfi, 2006), which contains the same algorithms of the original Simqke code (Vanmarcke and Gasparini, 1976).

4 Energy-based ground motion parameters

For each selected set of real, modified and artificial accelerograms, different energy-based GMPs are obtained in order to evaluate if the manipulation or the generation of time histories generates unrealistically high energy contents of the signals, thus influencing the corresponding seismic demand. The considered GMPs are the following:

- Arias Intensity (AI): AI (Arias, 1970) is an index for the energy content of ground motions that incorporates both the duration and the amplitude of the entire ground motion time history. AI is defined in Eq. (2), where $a(t)$ is the ground motion acceleration at time t, t_{max} is the total duration of the ground motion, and g is the gravity acceleration:

$$AI = \frac{\pi}{2g}\int_0^{t_{max}} a^2(t)dt \quad (2)$$

- Specific Energy Density (SED): SED is the integral of the square velocity time history $v(t)$ over the entire time range, as indicated in Eq. (3):

$$SED = \int_0^{t_{max}} v^2(t)dt \quad (3)$$

- Cumulative Absolute Velocity (CAV): the Electric Power Research Institute (EPRI) introduced CAV as a potential ground motion intensity measure for the identification of the structural damage (Reed and Kennedy, 1988). The most commonly used definition of CAV is defined in Eq. (4):

$$CAV = \int_0^{t_{max}} a(t)\,dt \quad (4)$$

- Acceleration Spectrum Intensity (ASI): ASI was defined by Von Thun et al. (1988) as the area under the response acceleration spectrum (ranged from 0.1 to 0.5 s) as indicated in Eq. (5), where S_a is the pseudo-acceleration, ξ is the damping coefficient, and T is the fundamental period of vibration.

$$\mathrm{ASI} = \int_{0.1}^{0.5} S_a\left(\xi = 5\%, T\right) dT \tag{5}$$

- Housner Intensity (HI): Housner (1952) proposed a measure of the damage potential of an earthquake characterized by the area (between 0.1 and 2.5 s) under the pseudo-velocity spectrum, as shown in Eq. (6), where S_V is the pseudo-velocity spectrum.

$$\mathrm{HI} = \int_{0.1}^{2.5} S_V\left(\xi = 5\%, T\right) dT \tag{6}$$

Figure 4a and Figure 4b show the ratios between the energy based GMPs calculated for SMR-RR and RR and obtained for the bare and the infilled structure, respectively. The two plots indicate that the spectral matching process significantly modify the energy content of the real records, especially in terms of AI and SED: for several records the maximum $GMP_{SMR\text{-}RR}/GMP_{RR}$ ratios (Max_{GMPs}) are greater than 10. On average, for both structural models the ratios of the GMPs obtained before and after the spectral matching process are between 3 and 4 for AI (Avg_{AI}) and SED (Avg_{SED}) and between 1 and 2 of the other GMPs (Avg_{CAV}, Avg_{ASI} and Avg_{HI}).

Similarly, Figure 5a and Figure 5b report the ratios between the energy based GMPs calculated for SMR-LS and LSR and obtained for the bare and the infilled structure, respectively. In this case, both maximum (Max_{GMPs}) and average ratios of GMPs (Avg_{GMPs}) are significantly lower than those shown in Figure 4, and specifically $0.17 \leq Max_{GMPs} \leq 9.63$ and $1.04 \leq Avg_{GMPs} \leq 2.00$. This shows that the spectral-matching process generates in general a great modification of GMP, but this effect can be mitigated if the matching process is carried out using sets of accelerograms characterized by a reduced spectral variability, as for example the spectrum-compatible linearly scaled ground motion records (LSR).

The comparison between the GMPs obtained from AA and RR (Figure 6) was carried out calculating the ratios between the GMPs obtained from each artificial accelerograms (GMP_{AA}) and the average GMPs obtained from RR ($GMP_{Avg\text{-}RR}$). On average, the artificial accelerograms have a higher energy content than real records, especially in terms of AI, for which $Avg_{AI} = 2.42$.

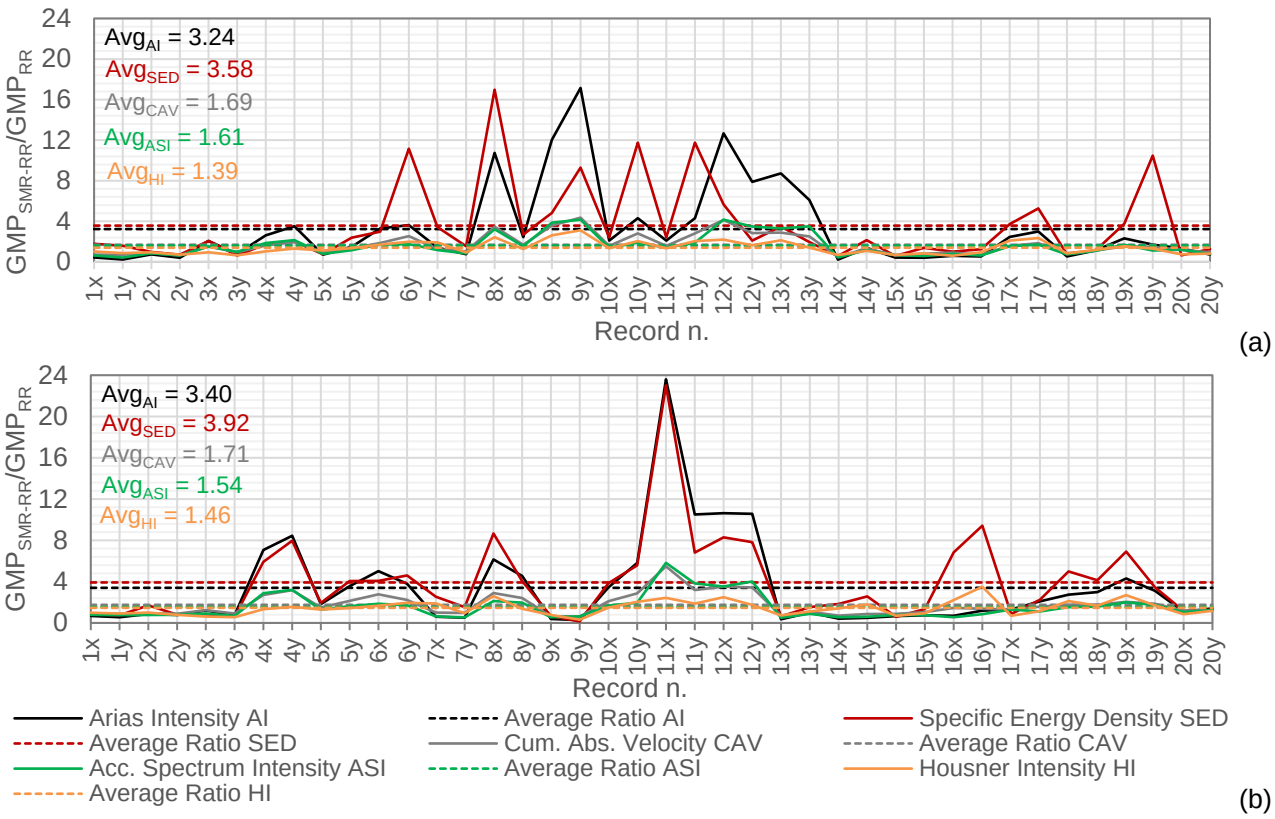

Figure 4. Ratios between the energy-based GMPs of SMR-RR and RR obtained for the bare (a) and the infilled (b) structure.

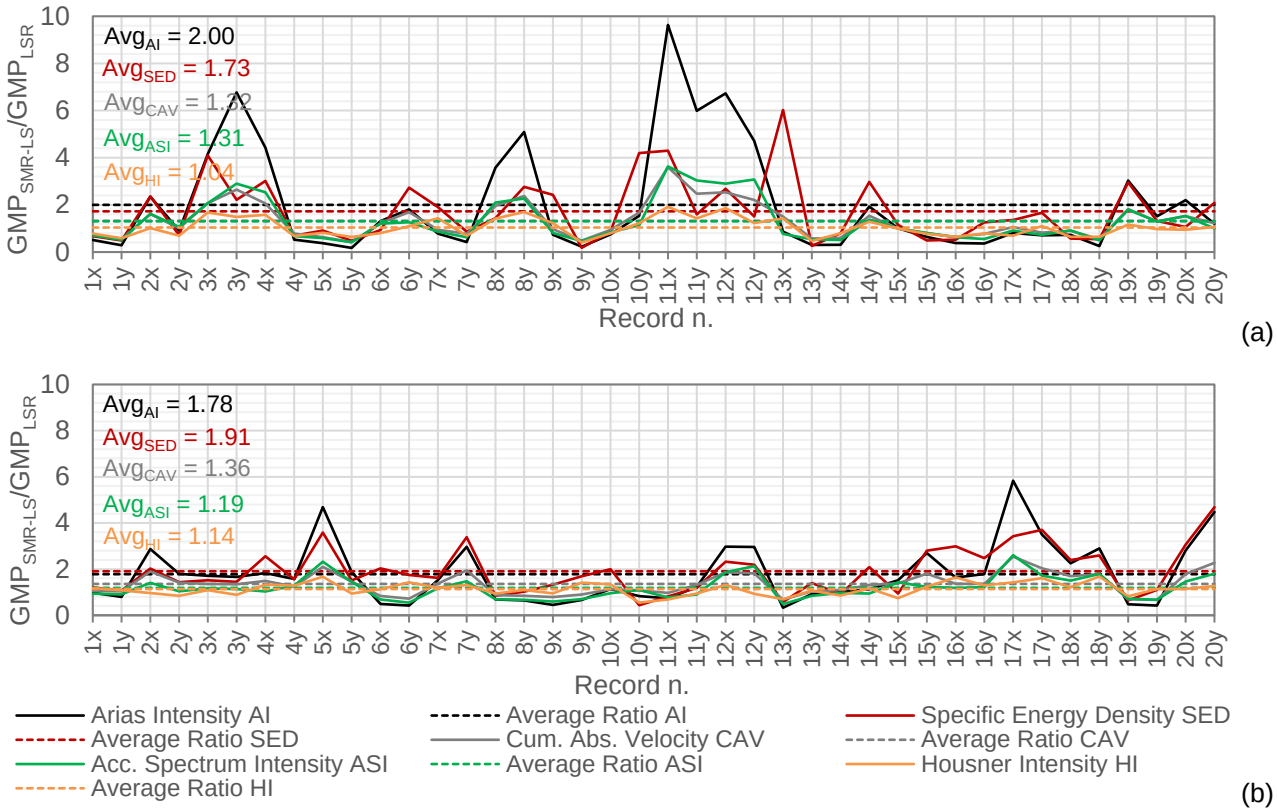

Figure 5. Ratios between the energy-based GMPs of the spectral matched records SMR-LS and the corresponding linearly scaled ground motion records (LSR) obtained for the bare (a) and the infilled (b) structure.

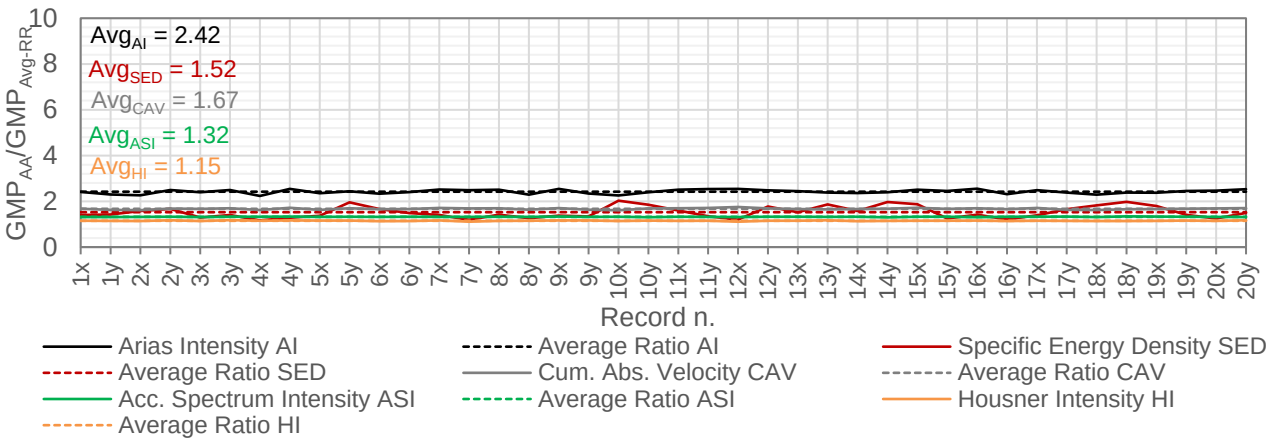

Figure 6. Ratios between the GMPs obtained from AA (GMP$_{AA}$) and the average GMPs obtained from RR (GMP$_{Avg-RR}$).

5 Results and comparisons

The bare structure and the infilled structure were analysed with NRHAs using the four different ground motion sets described in Section 3 (RR, SMR-RR, SMR-LS and AA). For each pair of selected ground motion records, the Roof Drift Ratios (RDRs) in the x- and y-directions were obtained as the roof displacements normalized with respect to the total height of the structure. For both x- and y- structural directions, the ratios of the RDRs obtained before and after the spectral matching process were computed next. More specifically, Figure 7a and Figure 7b show the RDRs obtained for the bare structure real unscaled records (RR) or linearly scaled records

(LSR), respectively. The black and grey bars represent the results in the x- and y-directions, respectively, while the horizontal lines represent the corresponding average RDR ratios (Avg-x and Avg-y). Figure 8a and Figure 8b report the same results for the infilled structure. RDRs obtained from non-convergent analyses were not considered. For artificial accelerograms, the ratios between the RDRs obtained from the generated record and the average RDR obtained from the RR are reported in Figure 9.

The results of the NRHAs indicate that the maximum RDR ratios ($Max_{RDRratio}$) are very high when the infilled structure using SMR-RR is analysed ($Max_{RDRratio\_x}$ = 6.87 and $Max_{RDRratio\_y}$ = 5.89). On average, RDR_{SMR-RR}/RDR_{RR} is greater than RDR_{SMR-LS}/RDR_{LSR} . This indicates that if the spectral matching process is carried out on scaled accelerograms, it produces a reduced variation of the Engineering Demand Parameter (EDP).

The ratios between the RDRs obtained from artificial and real accelerograms are almost constant for all the 20 pairs of ground motion records. For the bare structure, the average ratios in the x- and y-directions (Avg-x and Avg-y) are equal to 1.29 and 1.09, respectively; for the infilled structure these ratios assume lower values as they are equal 1.45 and 1.43, respectively.

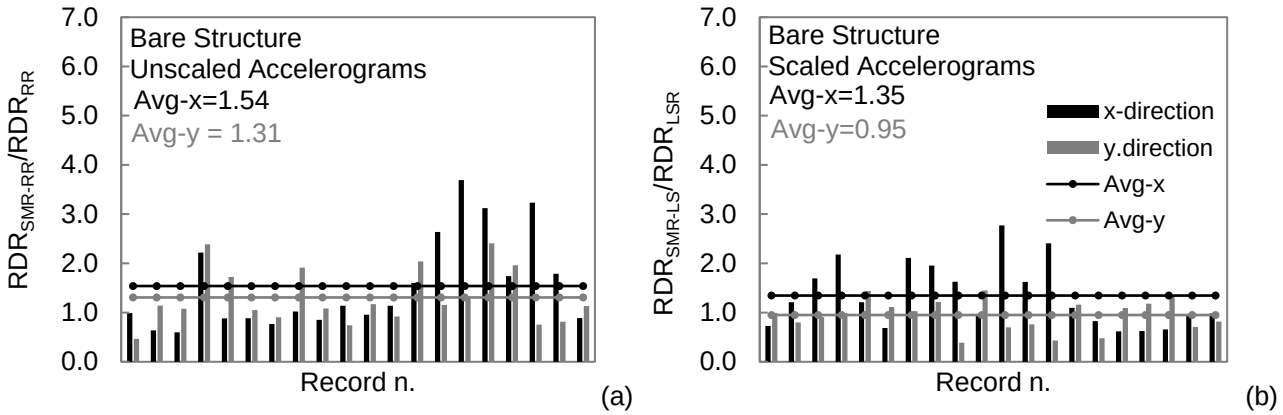

Figure 7. Ratios between the RDRs obtained from the bare structure using SMR-RR and RR (a) and SMR-LS and LSR (b).

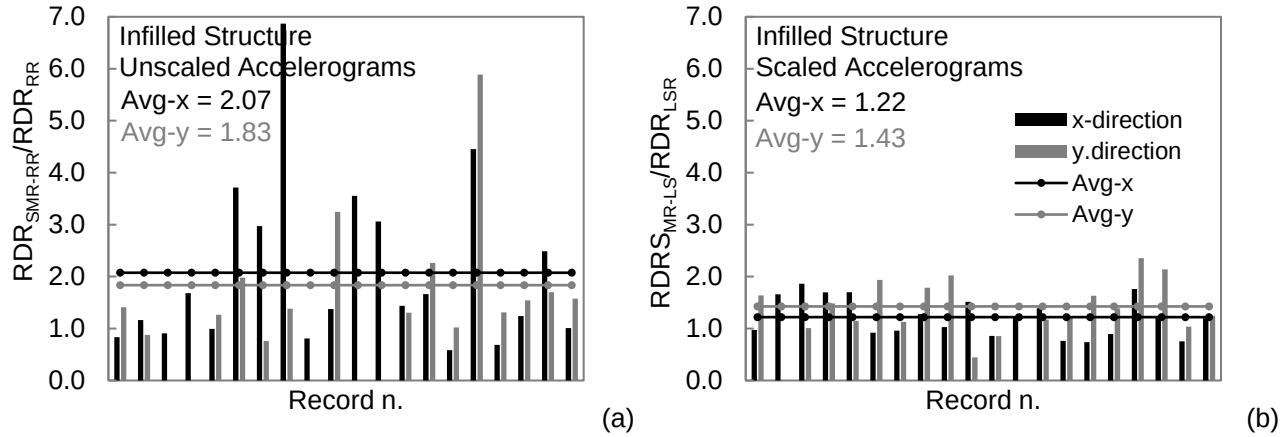

Figure 8. Ratios between the RDRs obtained from the infilled structure using SMR-RR and RR (a) and SMR-LS and LSR (b).

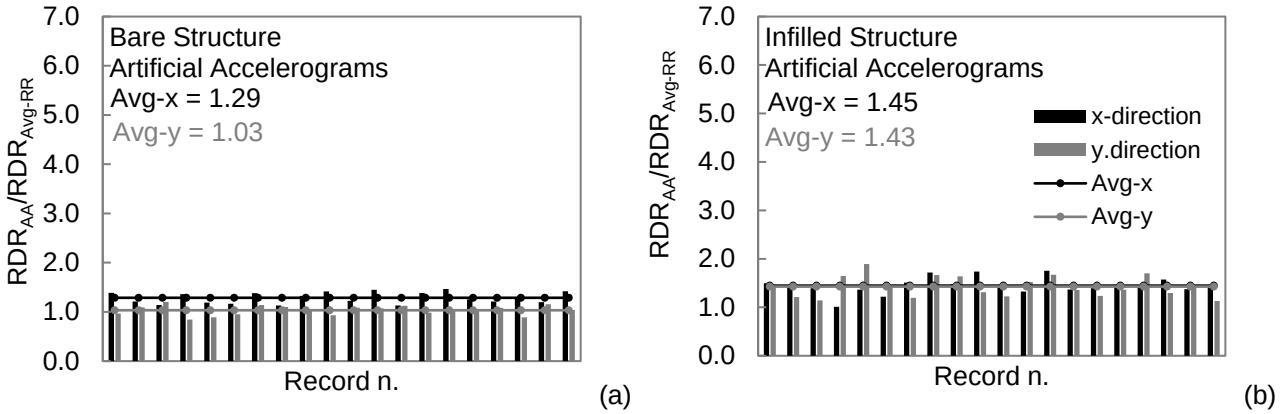

Figure 9. Ratios between the RDRs obtained from AA (RDR_{AA}) and the average RDRs obtained from RR (RDR_{Avg-RR}) for the bare structure (a) and the infilled structure (b).

6 Conclusions

This paper aims at evaluating the effects of the modification and generation of ground motions on the energy content of the seismic input and on the EDP obtained from NRHAs. Different sets of spectrum-compatible ground motions records were selected: real unscaled ground motion records RR, linearly scaled ground motion records LSR, spectral-matched ground motion records obtained from real records SMR-RR or linearly scaled records SMR-LS and artificial accelerograms AA. For each of these record group, several energy based GMPs were calculated (AI, SED, CAV, ASI and HI) in order to evaluate the variation of the energy content of the ground motions due to the spectral matching process or to the generation of the accelerograms. NRHAs of a six-story existing RC structure were then carried out with different groups of selected time histories and for each ground motion record, the corresponding RDR was obtained. The main outcomes of the study are summarized hereafter:

- The spectral-matching process carried out on real unscaled accelerograms (RR) generates a significant modification of the energy content of the ground motion records. However, this variation can be significantly attenuated if the spectral-matching process is carried out after a linear scaling of the ground motion records.
- The comparison between the GMPs obtained between AA and RR show that the generation of artificial accelerograms produces on average time histories with a high energy content, especially in terms of AI, for which the average ratio GMP_{AA}/GMP_{Avg-RR} is equal to 2.42. If all GMPs are considered, on average, the AAs are characterized by an energy content that is 60% higher than that of RR.
- When the case-study structure is analysed using SMR, the RDRs are significantly higher than those obtained from the corresponding unmodified ground motions. On average, the ratios between the RDRs obtained before and after the spectral matching process in the x- and y-directions (Avg-x and Avg-y) assume the highest values when the infilled structure is analysed using spectrum-compatible RR. In this case, Avg-x = 2.07 and Avg-y = 1.83. When the spectral matching process is carried out using LSR, the effects of the ground motion modification on the seismic demand is significantly mitigated due to the reduced spectral variability of LSR. On average, the ratios between the RDRs obtained from SMR-LS and LSR in the two structural directions x and y are in this case equal to 1.35 and 0.95 for the bare structure and 1.22 and 1.43 for the infilled structure.
- The RDRs obtained from the AA are higher than those obtained from RR. Specifically, for the infilled structure, on average the RDRs obtained from AA are more than 40% higher than those obtained from RR.

Future developments of the work could include the analysis of spectrum-compatible records to a seismic hazard corresponding to different return periods in order to analyse the effect of the ground motion selection process on the seismic demand with increasing structural non-linearities.

7 References

Cantagallo C., Camata G., Spacone E. (2014). Seismic demand sensitivity of reinforced concrete structures to ground motion selection and modification methods, *Earthquake Spectra*, 30(4): 1449-1465. doi: 10.1193/062812EQS226M.

Romanelli, F., Vaccari, F., Cantagallo, C., Camata, G. and Panza, G. F. (2023). Physics-Based Approach to Define Energy-Based Seismic Input: Application to Selected Sites in Central Italy. In *International Workshop on Energy-Based Seismic Engineering*, Springer Nature Switzerland, 112-128. doi: 10.1007/978-3-031-36562-1_9.

Ministero dei lavori pubblici, Decreto Ministeriale del 30/05/1974 (DM 30/05/1974), Norme tecniche per la esecuzione delle opere in cemento armato normale e precompresso e per le strutture metalliche, Gazzetta Ufficiale Serie generale n. 198 del 29/07/1974, Roma (in Italian).

Ministero dei lavori pubblici, Decreto ministeriale del 16/01/1996 (DM 16/01/1996), Norme tecniche relative ai «Criteri generali per la verifica di sicurezza delle costruzioni e dei carichi e sovraccarichi», Gazzetta Ufficiale Serie generale n. 29 del 5/02/1996, Roma (in Italian).

McKenna F., Scott M.H., Fenves G.L. (2010) Nonlinear finite-element analysis software architecture using object composition, *Journal of Computing in Civil Engineering*, 24(1):95-107. doi: 10.1061/(ASCE)CP.1943-5487.0000002

Petracca M., Candeloro F., Camata G. (2017) STKO user manual. ASDEA Software Technology, Pescara.

Scott M.H., Fenves G.L. (2006) Plastic Hinge Integration Methods for Force-Based Beam-Column Elements, *Journal of Structural Engineering*,132(2):244-252. doi: 10.1061/(ASCE)0733-9445(2006)132:2(244).

Spacone E, Filippou FC, Taucer FF. Fibre beam‐column model for non‐linear analysis of R/C frames: Part I. Formulation. *Earthquake Engineering & Structural Dynamics* 1996; 25(7):711-725. doi: 10.1002/(SICI)1096-9845(199607)25:7<711::AID-EQE576>3.0.CO;2-9.

Terrenzi, M., Spacone, E. and Camata, G. (2020). Comparison between phenomenological and fiber-section non-linear models. *Frontiers in Built Environment*, 6, 38. doi: 10.3389/fbuil.2020.00038.

Kent D.C., Park R. (1971) Flexural members with confined concrete, *Journal of the Structural Division*, ASCE; 97:ST7. doi: 10.1061/JSDEAG.0002957

Mazzoni S., McKenna F., Scott M.H., Fenves G.L. (2006) OpenSees command language manual, Pacific Earthquake Engineering Research (PEER) Center, 264:137-158.

Barbagallo F., Bosco M., Marino E.M., Rossi P.P. (2020) On the fibre modelling of beams in RC framed buildings with rigid diaphragm, *Bulletin of Earthquake Engineering*, 18(1):189-210. doi: 10.1007/s10518-019-00723-z.

Ambraseys N., Smit P., Dougles G., Margaris B., Sigbjornsson R., Ólafsson S., Suhadolc P., Costa G. (2004) Internet-Site for European Strong-Motion Data, European Commission, *Bollettino di geofisica teorica ed applicata*, 45(3): 113-129.

Luzi L., Puglia R., Russo E. (2016) ORFEUS WG5. Engineering Strong Motion Database, version 1.0. Istituto Nazionale di Geofisica e Vulcanologia, *Observatories & Research Facilities for European Seismology*. doi:10.13127/ESM.

Cantagallo C., Camata G., Spacone E. (2015) Influence of ground motion selection methods on seismic directionality effects, *Earthquakes and Structures*, 8(1): 185–204. doi: 10.12989/eas.2015.8.1.185.

Skoulidou D.; Romão X. (2020) The significance of considering multiple angles of seismic incidence for estimating engineering demand parameters. *Bull. Earthq. Eng.*, 18:139–163. doi: 10.1007/s10518-019-00724-y.

Cantagallo C., Terrenzi M., Spacone E. and Camata G. (2023) Effects of Multi-Directional Seismic Input on Non-Linear Static Analysis of Existing Reinforced Concrete Structures, *Buildings*, 13(7): 1656. doi: 10.3390/buildings13071656.

CEN (2005). *EN 1998-1:2005. Eurocode 8: Design of structures for earthquake resistance - Part 1: General rules, seismic actions and rules for building*, Comité Européen de Normalisation, Brussels.

Beyer K., Bommer, J.J. (2006). Relationships between median values and between aleatory variabilities for different definitions of the horizontal component of motion, *Bulletin of the Seismological Society of America*, 96(4A): 1512-1522. doi:10.1785/0120050210.

Hancock J., Watson-Lamprey J., Abrahamson N. A., Bommer J. J., Markatis A., McCoy E. M. M. A. and Mendis, R. (2006). An improved method of matching response spectra of recorded earthquake ground motion using wavelets. *Journal of Earthquake Engineering*, 10(spec01), 67-89.

Seismosoft (2022) A Computer Program for Spectrum Matching of Earthquake Records (2022). Available from URL: https://seismosoft.com/

Al Atik L. and Abrahamson N. (2010). An improved method for nonstationary spectral matching. *Earthquake spectra*, *26*(3), 601-617.

Gelfi P. (2006) SIMQKE_GR. Artificial earthquakes compatible with response spectra, University of Brescia, Italy.

Vanmarcke E. H. and Gasparini D. A. (1976) SIMQKE: A program for artificial motion generation, *Rep. No. R76-4*, Dept. of Civil Engineering, Massachusetts Institute of Technology, 99.

Arias A (1970) A measure of earthquake intensity. In: Hansen RJ (ed.) Seismic Design for Nuclear Power Plants. Cambridge, MA: MIT Press, pp. 438–483.

Reed J.W. and R.P. Kennedy (1988). A Criterion for Determining Exceedance of the Operating Basis Earthquake, *EPRI Report NP-5939*, July 1988.

Von Thun J.L., Rochim L.H., Scott G.A., Wilson J.A. (1988) Earthquake ground motions for design and analysis of dams, *Earthquake Engineering and Soil Dynamics* II - Recent Advances in Ground-Motion Evaluation, Geotechnical Special Publication, 20, pp. 463-481.

Housner, G.W. (1952). Spectrum Intensities of Strong-Motion Earthquakes. In *Proceedings of the Symposiumon Earthquake and Blast Effects on Structures*, EERI, Oakland California, 20–36.

Decanini, L. D., & Fantin, G. E. (1986). Modelos simplificados de la mampostería incluida en porticos. Caracteristicas de stiffnessy resistencia lateral en estado limite. Jornadas Argentinas de Ingeniería Estructural, 2, 817-836.

Cardone, D., & Perrone, G. (2015). Developing fragility curves and loss functions for masonry infill walls. Earthquakes and Structures, 9(1), 257-279

Sassun, K., Sullivan, T. J., Morandi, P., & Cardone, D. (2016). Characterising the in-plane seismic performance of infill masonry. Bulletin of the New Zealand Society for Earthquake Engineering, 49(1), 98-115.